Correlation of Experimental and Theoretical Results for Vaporization by Simulated Disruption

C.D. Croessmann, G.L. Kulcinski and J.B. Whitley

May 1984

UWFDM-576

J. Nucl. Materials 128 & 129, 816 (1984).

FUSION TECHNOLOGY INSTITUTE

UNIVERSITY OF WISCONSIN

MADISON WISCONSIN

Correlation of Experimental and Theoretical Results for Vaporization by Simulated Disruption

C.D. Croessmann, G.L. Kulcinski and J.B. Whitley

Fusion Technology Institute
University of Wisconsin
1500 Engineering Drive
Madison, WI 53706

http://fti.neep.wisc.edu

May 1984

UWFDM-576

J. Nucl. Materials 128 & 129, 816 (1984).

CORRELATION OF EXPERIMENTAL AND THEORETICAL RESULTS FOR VAPORIZATION BY SIMULATED DISRUPTION

by

C.D. Croessmann and G.L. Kulcinski
Fusion Engineering Program
Nuclear Engineering Department
University of Wisconsin
Madison, WI 53706 USA

and

J.B. Whitley
Sandia National Laboratories
Albuquerque, NM 87185 USA

May 1984

UWFDM-576

Abstract

Samples of Al, 1100 Al, SS 304, Ni, Mo, and TZM were subjected to a simulated plasma disruption produced by a 25 kV electron beam for times of 100 to 500 msec with an energy flux of 0.5 to 7.0 kJ/cm^2. The net vaporized thickness was measured as a function of absorbed energy density for experimental results and predicted by theoretical models. Agreement was found for the threshold energy density for vaporization and the functional dependence of vaporization on energy density over a wide range of parameters. The usefulness of electron beam experiments to verify and guide the development of vaporization models for high heat flux component design was shown.

Introduction

The inner components of a fusion reactor, such as the first wall, limiters, and rf antenna, will be subjected to an intense thermal load during a severe plasma disruption. The amount of vaporization of surface materials that results will be a key factor in determining component lifetime and plasma contamination. Extensive theoretical efforts [1-5] have been made to quantify this process so that high heat flux surfaces can be best designed for thermal response. However, depending upon the vaporization model and the assumed disruption conditions, the predicted vaporization thickness can vary by over an order of magnitude [6].

The use of high energy electron beams to simulate lower energy plasma disruptions has been questioned since the range of electrons in metals (1-5 μm for 25 keV) differs from that of D or T ions (.1 μm for 10 keV). The motive of this study was to produce a body of experimental data that could address this question and then be used to verify and enhance existing analytical models and suggest further areas of study. Using a rastered electron beam, a variety of materials were subjected to a rapid and intense heat flux. The results, plotted as net vaporized thickness of material vs. energy density, can be compared directly to theoretical predictions for the same thermal conditions.

One analytical model, developed at the University of Wisconsin to predict evaporation, is briefly outlined. The experimental procedure is given and the data is compared to the predictions.

Analytical Methods

The predicted vaporization thickness of a material subjected to a given disruption scenario was obtained with a finite-difference computer code,

SOAST. This code was based upon the time and space dependent heat conduction equations and solution development suggested by Hassanein [4]. The result was a time varying one dimensional temperature distribution which took into account the double moving-boundary problem of the vapor-liquid and liquid-solid interfaces.

The thermophysical properties of the material were treated as functions of the local temperature and the back surface was assumed to be held at a constant temperature. The energy incident on the front surface was distributed into conduction, melting, evaporation, and radiation. The heat flux was assumed to be a square pulse in time. The vaporization model considered the time dependent kinetics by utilizing transport theory. Temperature dependent vapor pressure relations were used to consider the vaporization and recondensation processes which occurred in the vapor layer. Also, the interaction of the vapor with the incoming particles was considered.

The vapor layer thickness that develops will increase with time during a disruption. Therefore, an increasing number of the energetic particles will deposit their energy in the vapor layer before reaching the condensed wall material. This energy was assumed to be isotropically reradiated, with the result that the heat flux deposited on the condensed phases was reduced. When the vapor thickness exceeded the range of the energetic particles in the material, all of the original monodirectional energy was first deposited in the vapor layer; thus the first wall received only one half of the reradiated isotropic energy flux. This simple model assumed that after reradiation, the energy did not interact with the vapor and that all of the vapor remained near the condensed phases to act as a shield. Complete details of the equation,

boundary conditions, vaporization model, and solution methods are discussed elsewhere [4,7].

For comparison with the experimental data, three theoretical curves were produced giving net evaporated thickness as a function of deposited energy density. The first considered the most severe vaporization, which would result if all of the vapor layer was removed as it was produced. In this unshielded case, all of the energy flux was deposited directly upon the condensed material. The second case distributed the incident energy over the depth of penetration of the energetic electrons in the vapor. While this did not treat the electron energy deposition in an exact manner, it was important in determining the usefulness of electron beams as a simulation technique. The third case utilized the range of 10 keV deuterons in the material as part of the shielding. This plasma shielding was given as a reference to reactor technology and as an optimistic prediction. Thus the three curves given in all of the results represent the worst and best case scenarios for this model with a more experimentally realistic median.

Experimental Procedure

Six different materials were used in the rapid vaporization testing conducted at the Electron Beam Test Facility (EBTF) at Sandia National Laboratories - Albuquerque. The samples were solid cylinders, 1.27 cm in height and 0.635 or 0.952 cm in diameter as shown In Table 1. The variation in sample diameter was due only to the stock readily available. A total of 250 samples were tested.

The top surface of each sample was mechanically polished to a 600 grade finish to remove machining marks. Each sample was placed in an ultrasonic cleaner in sequential baths of trichloroethylene, isopropyl alcohol, 50%

Table 1. Summary of Vaporization Samples and the Associated Thermal Test Conditions.

Material	Number of Samples	Sample Diameter (cm)	Test Duration (msec)	Range of Energy Flux (kJ/cm^2)
pure Al	9	0.635	100	0.8-1.4
1100 Al	25	0.952	100	0.5-1.6
SS 304	13	0.635	100	1.2-2.0
	21		200	1.0-2.9
Nickel	19	0.952	300	1.9-3.5
Molybdenum	17	0.635	400	3.2-5.8
TZM	9	0.952	500	4.9-6.4

isopropyl alcohol/deionized water, and deionized water each for a duration of greater than 2 minutes. Dry air was used to remove remaining water. Each sample was weighed to an accuracy of ± 10 μg.

Samples were placed in a graphite grid holder which could accommodate 32 pieces in a 4 x 8 arrangement. The grid size was 30 cm by 16 cm with a 1.0 cm height. The 32 placement holes were tapped through the holder to provide a tight lateral thermal contact between the graphite and the samples. Graphite was used to force a more unidirectional heat transport since its thermal response is much slower than the metal samples.

The graphite holder and an enclosed load of samples were then placed upon a water-cooled copper stage (20°C) inside the EBTF. The electron beam gun was positioned vertically over the stage in a stationary position. The stage was motorized with computer controlled indexing of samples so that the specimen to be tested could be placed under the electron beam spot. The distance from the steering filaments of the gun to the sample was approximately 30 cm.

The electron gun itself was a 30 kW, 30 kV device with a beam rastered (400 Hz) over a 1 cm^2 area. The beam was roughly 1/2 cm at FWHM. A sample, placed in the center of the rastered area, intersected a nearly flat energy deposition profile due to the broad beam and the rapid raster rate.

The diagnostics of the facility included: a TV monitoring system with video recorder, a high speed movie camera with a 10000 frame/sec maximum speed, an optical pyrometer to record sample surface temperatures and residual gas analysis of the species evolved. Discharge and control of the electron gun as well as data acquisition were computer controlled. The computer generated a listing of all pertinent machine parameters and plots of electron gun power and sample surface temperature as functions of time [8].

The EBTF was calibrated for the vaporization experiments by using a copper slug calorimeter, a solid cylinder the size of the test specimens with an embedded thermocouple. The calorimeter was mounted in the graphite holder and subjected to a wide range of energy flux loads. No phase change was allowed to occur. The result was a set of curves of energy produced by the electron gun (calculated by controlling computer) vs. energy flux on the calorimeter for various pulse times. Thus, for each experimental shot the energy flux on the test sample could be determined within the experimental error of the calorimetry. Note that no attempt was made to correct the energy deposition calibration for the atomic number of the target.

Each material experienced a wide range of test conditions, as shown in Table 1, but each sample was tested only once. After the vaporization tests were completed, the samples were recleaned using the previously described method and reweighed. The weight loss of each sample was translated into net vaporized thickness.

Results

Figure 1 shows the net vaporized thickness of aluminum as a function of energy density for 100 msec shots. Data from pure aluminum and 1100 aluminum alloy samples are shown including representative error bars. For a given energy density the 1100 Al consistently had a smaller vaporized thickness than the pure Al. Also shown are three theoretical curves as previously described. Because the range of electrons in aluminum is numerically larger than the values of vaporized thickness shown, the electron vapor shielding model gives results quite close to those of the unshielded case. When the vaporized thicknesses near the value of the range (> 4.5 μm), the electron shielding curve should approach the plasma shielding curve. The predicted threshold

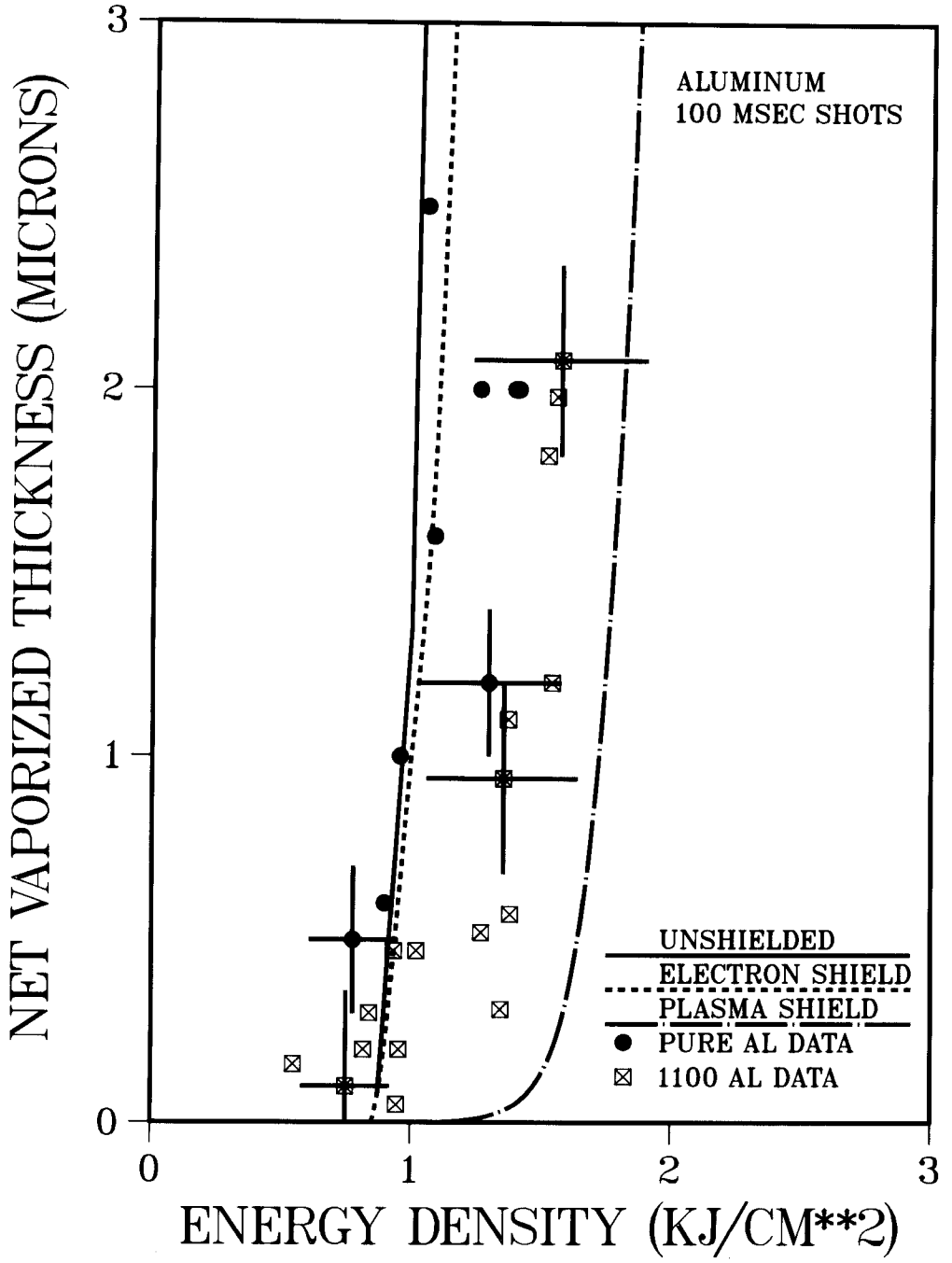

Fig. 1. Comparison of theoretical and experimental results with representative error bars for pure Al and 1100 Al after 100 msec shots.

energy density for vaporization is slightly larger than what is experimentally observed, but at higher energy densities the theory bands the experimental data quite well.

Figures 2 and 3 show the vaporization results from SS 304 samples subjected to 100 msec and 200 msec heat fluxes respectively. The data is self-consistent and agrees with the slope of the predicted curves. However, the data also indicates that less vaporization occurs from these samples than is predicted by the computer model. Note that a slight knee occurs in the curve for the electron shield case. This occurs when the vaporized thickness approaches and exceeds the range of electrons in the steel.

As seen in Fig. 4, the data for nickel samples after 300 msec shots is enclosed by the anticipated values. The electron shield model agrees with the data when the vaporized thicknesses are greater than the range of electrons in nickel (> 3 μm). In addition, the predicted threshold energy density is appropriate. For evaporated thicknesses less than the electron range the model overpredicts the amount of vaporization.

The results for molybdenum after 400 msec shots and TZM after 500 msec shots are shown in Fig. 5 and 6 respectively. Most of the data for these two materials are clustered at vapor thicknesses less than 1 micron. It was difficult to vaporize material of larger thicknesses; however, the few data points of greater than 1 micron verify the near vertical slope of the vaporization curve. The data and the predicted threshold for vaporization are in exceptionally good agreement for molybdenum. Again at small vaporization thicknesses the electron shield model overpredicts the material lost.

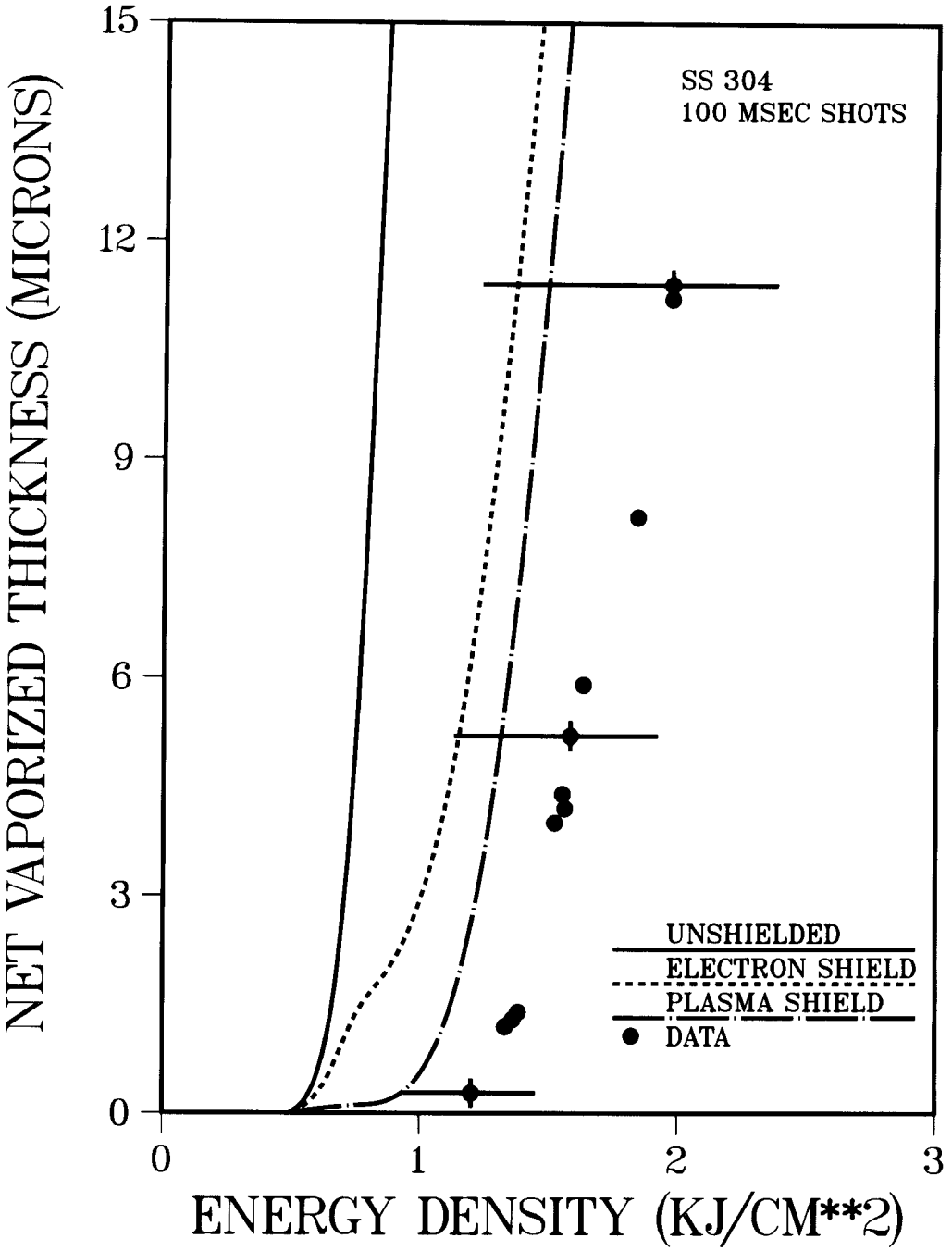

Fig. 2. Comparison of theoretical and experimental results for SS 304 after 100 msec shots. The error bars take into consideration changes in liquid surface area.

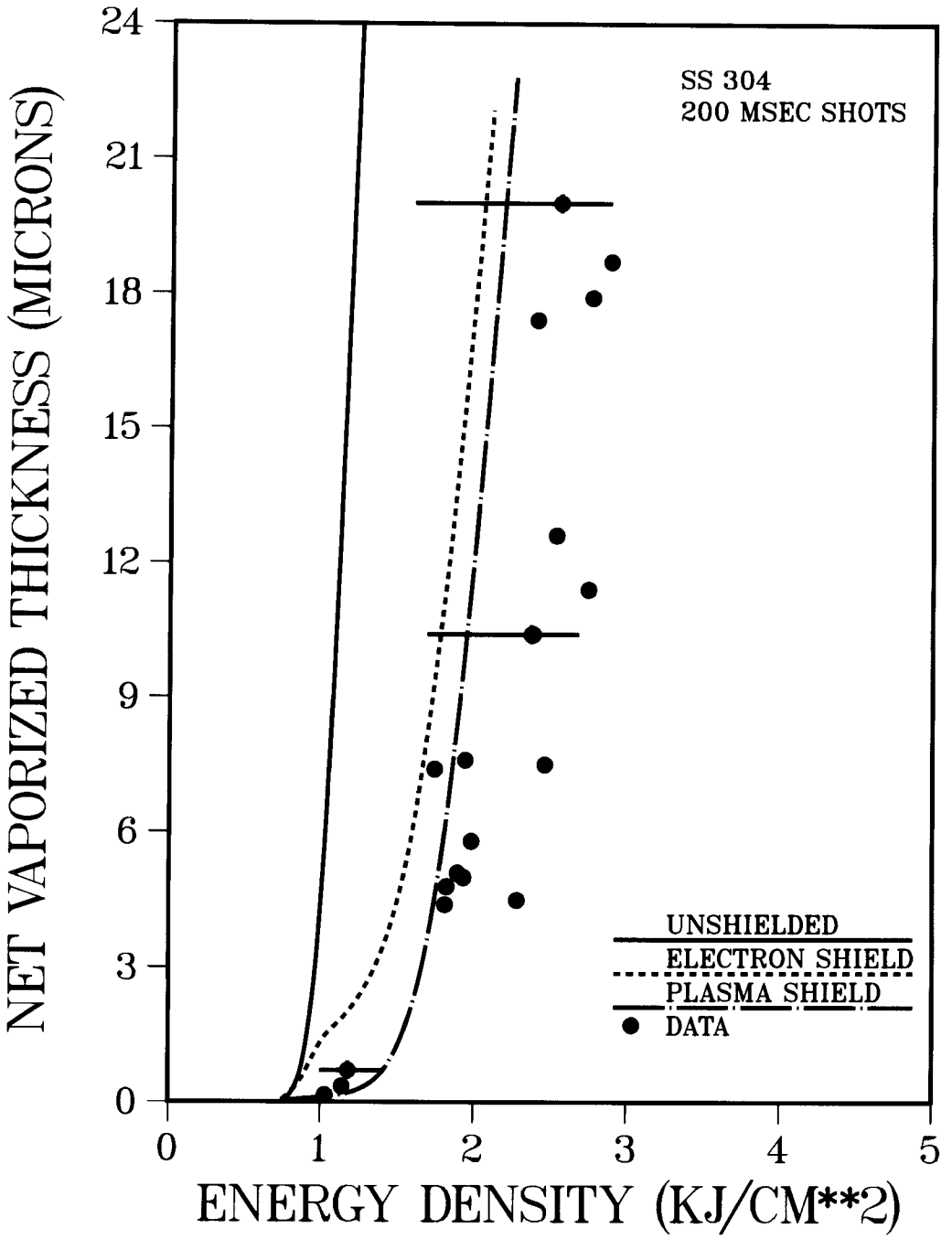

Fig. 3. Comparison of theoretical and experimental results for SS 304 after 200 msec shots. The error bars take into consideration changes in liquid surface area.

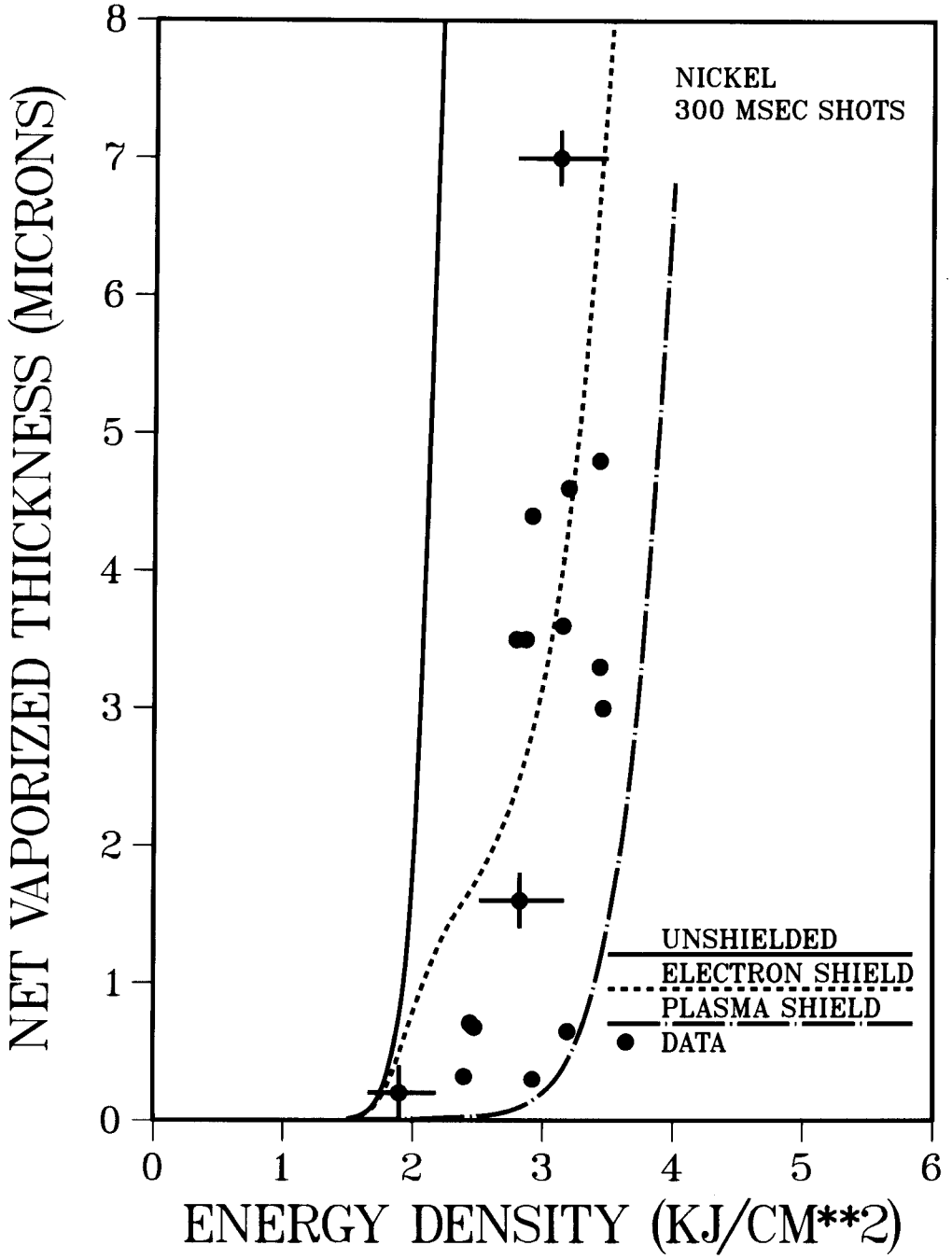

Fig. 4. Comparison of theoretical and experimental results for nickel after 300 msec shots.

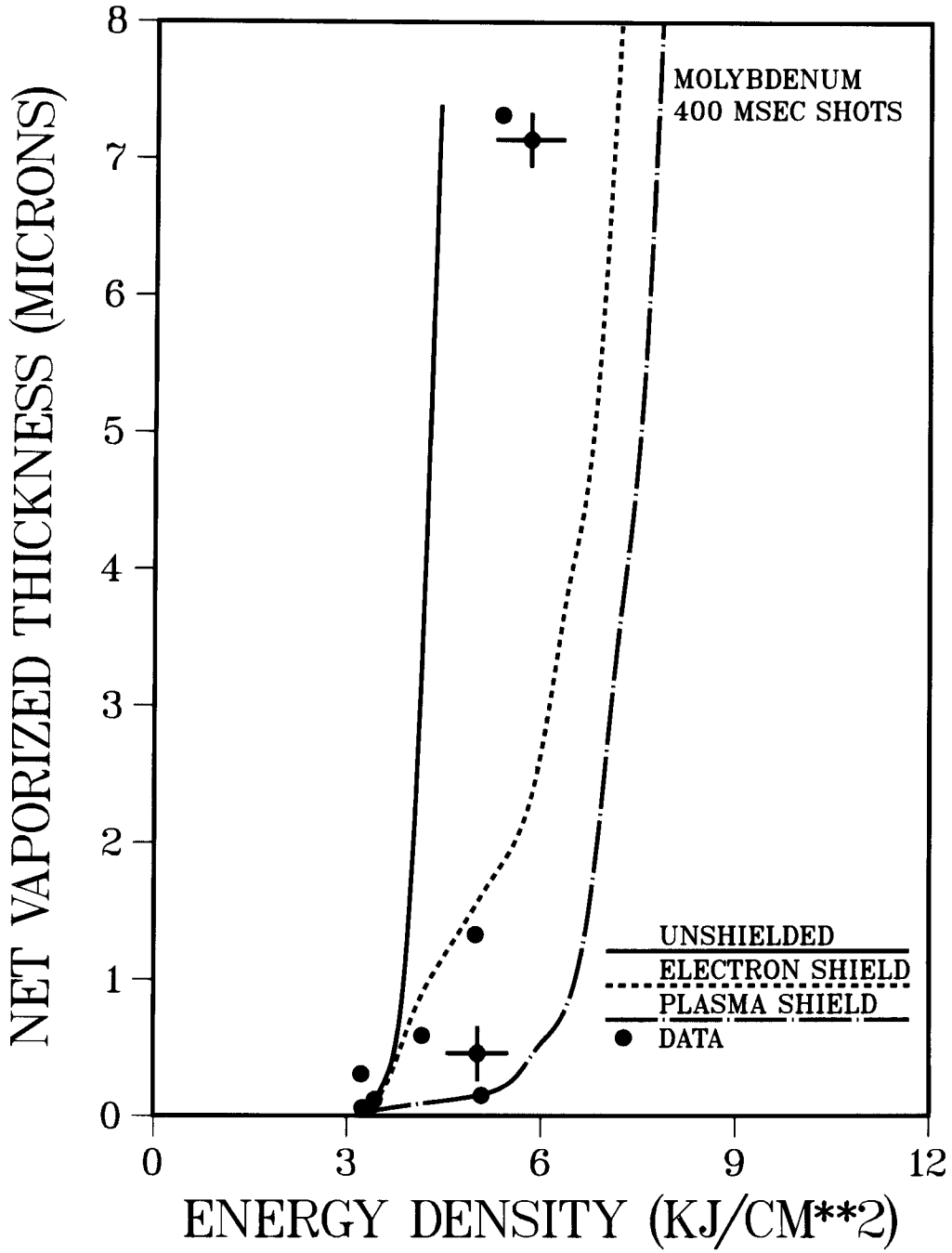

Fig. 5. Comparison of theoretical and experimental results for molybdenum after 400 msec shots.

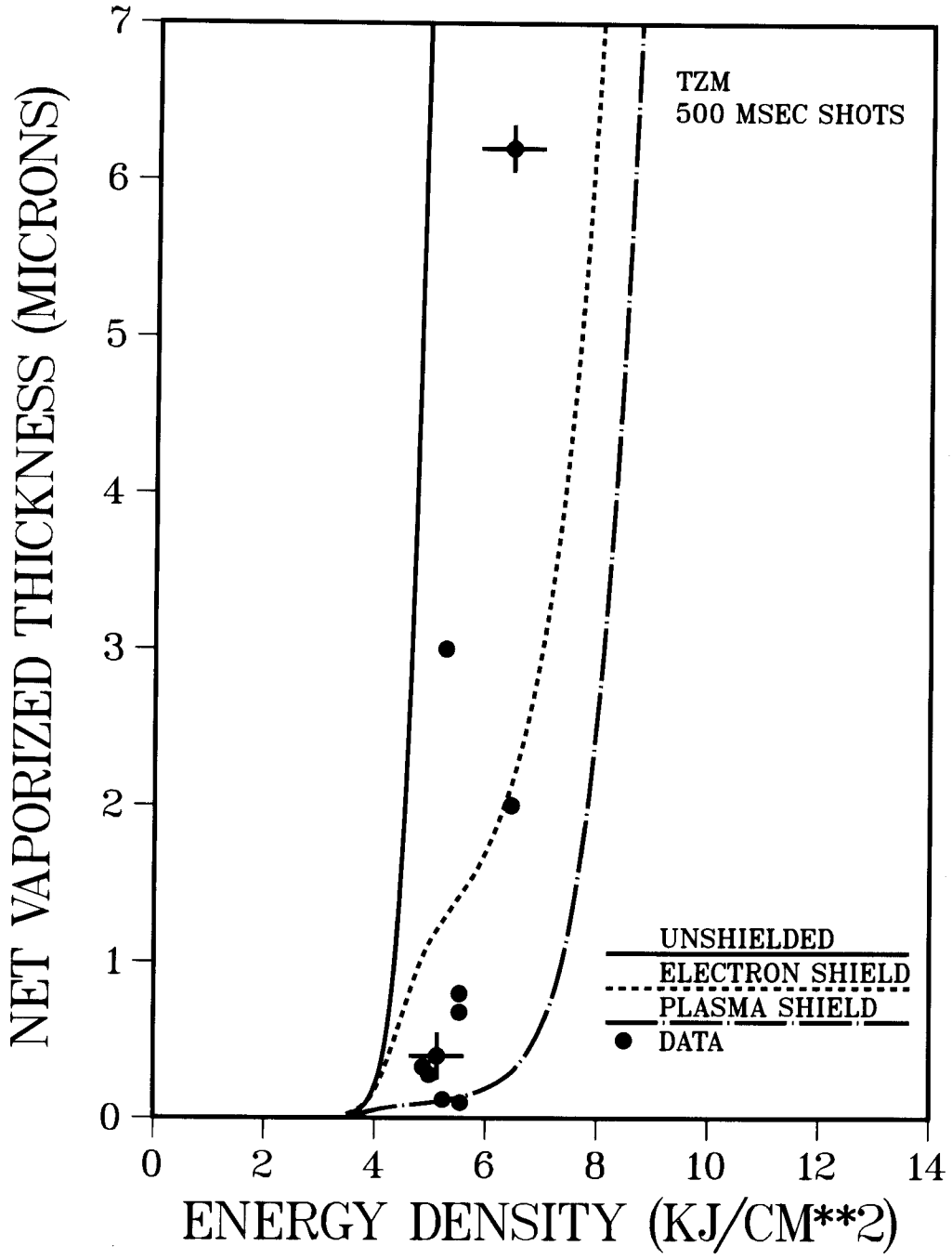

Fig. 6. Comparison of theoretical and experimental results for TZM after 500 msec shots.

Discussion

The scatter in the data and the representative error bars shown in all of the figures are due to experimental sources. First, the initial temperature of a sample, which significantly affects the vaporized thickness, varied slightly for each sample. This was due to variations in coolant water temperature and the heating of neighboring samples during a shot. Time was allowed between each shot to allow cooling of the system to minimize this effect. Secondly, to prepare for each shot the current of the electron gun filament was increased. This had the effect of preheating the samples. Precise alignment of a test sample in the beam raster area was difficult because of slippage in the motorized stage. Much time was spent improving each alignment using the line of sight through several ports. Finally the error of the weight measurements and the calibration of the absorbed energy flux must be considered.

As seen in Figs. 2 and 3, there was some disagreement between the experimental data and theoretical predictions for SS 304. This was attributed to a sizeable change in the liquid surface area during the SS 304 tests. After each test, the material that had melted had pulled into a symmetric conical shape on top of the sample with a cone height roughly equal to the radius of the cylinder. This phenomenon has been seen in other studies [9]. One possible explanation for this behavior is a magnetic field pinch effect created as the current goes through the sample. If this occurs during the discharge, the surface area of the condensed phase exposed to the energy flux may increase by some factor between 1 and 2 which changes as a function of time. This would then reduce the energy density on the sample during vaporization. The shift in the data is represented only in the error bars for the SS 304

since a more quantitative estimate of the energy density is not possible. The history of the surface area as a function of time would be needed to calculate the true energy density, but the qualitative direction of the shift is obvious. Each sample would also have a different surface area change since the quantity of melted material, and thus the size of the cone, varies sharply with increasing energy density. The other test materials also had surface modifications but they were much smaller in magnitude and any change in the energy density is already represented by their symmetric error bars.

The one-dimensional heat transport code and the experimental data agree across a broad range of heat pulse conditions. Since the samples were placed directly on top of a water cooled copper plate and encased in a material with a slow thermal response time, the heat transfer was directed primarily through the long axis of the cylinder during the pulse. It has been shown that the dimensional nature of the experimental setup and the spatial shape of the energy flux may strongly influence the vaporized thickness obtained with electron beam experiments of this type [10]. Because the beam was focused in a broad beam and rastered over an area larger than the sample, the heat flux across the sample surface was quite uniform. This was also necessary to allow the comparison of data to theory.

Care must be taken to insure that the electron beam experiment and model agree in the problem definition and assumptions. The vapor shield model must include the range of electrons in the material. With these considerations, the modified model and electron beam tests show reasonable agreement over a wide spectrum of cases.

The disruption times (100-500 msec) and the energy densities (0.5-7.0 kJ/cm^2) are considerably larger than those that are predicted for average

disruptions for a device such as INTOR (20 msec, 0.3 kJ/cm^2) [11]. The limits of the apparatus and the need for relatively large evaporation thickness for accurate measurements defined the lower range of the study's parameters. However, there are no cutoffs or limitations in the current vaporization models to prohibit their use with reactor type parameters. A more important concern is the presence of a magnetic field within the reactor which is not currently included in this model. The stability of the molten metal layer [12] and the motion of the metal vapor layer are only now being considered. In addition, rapid and intense heat loads may have significant effects on the thermophysical properties of alloys. Also an improved shielding model to account for energy deposition in the vapor and condensed phases is necessary to study second order effects.

Conclusions

The following conclusions can be drawn from this study:

1. Theoretical and experimental results give generally good agreement over a wide range of disruption conditions for a group of materials representing vastly different thermal and physical properties. The threshold energy density for vaporization and the increase in vaporization as a function of absorbed energy density agree with the SOAST model.
2. As is evidenced in all of the results except that of SS 304, some type of vapor shielding is reducing the severity of the energy flux and thus the vaporization. It is found that the simple shielding model used as a comparison in this study bands the data.
3. Electron-beam experiments, when properly treated, can be used to study the vaporization models as well as other related phenomena which are important to the design of high heat flux surfaces.

Acknowledgements

This work was performed under appointment to the Magnetic Fusion Energy Technology Fellowship program which is administered for the U.S. Department of Energy by Oak Ridge Associated Universities and with funds supplied by the Office of Fusion Energy, Department of Energy. In addition, the authors would like to thank Professor W.G. Wolfer of the University of Wisconsin for his interest and timely suggestions during this research.

References

[1] T.O. Hunter and G.L. Kulcinski, J. Nucl. Mater. 76/77 (1978) 383.

[2] R. Behrisch, J. Nucl. Mater. 93/94 (1980) 498.

[3] B.J. Merrill, Eng. Problems of Fus. Res. 11 (1981) 1621.

[4] A.M. Hassanein, Thermal Effects and Erosion Rates Resulting from Intense Deposition of Energy in Fusion Reactor First Walls, Ph.D. Thesis, Univ. of Wisconsin-Madison (1982) (UWFDM-465).

[5] T.H. Klippel, The Thermal Response of the First Wall of a Fusion Reactor Blanket to Plasma Disruptions, Netherlands Energy Research Foundation Report ECN-137 (1983).

[6] A.D. Bowers and J.R. Haines, J. Nucl. Mater. 103/104 (1981) 81.

[7] A.M. Hassanein, G.L. Kulcinski and W.G. Wolfer, Nucl. Eng. and Design/Fusion, to be published (also UWFDM-494).

[8] A.W. Mullendore, J.B. Whitley and D.M. Mattox, J. Nucl. Mater. 93/94 (1980) 486.

[9] J.R. Easoz et al., Nuclear Tech./Fusion 4 (1983) 780.

[10] A.M. Hassanein, Modeling the Interaction of High Power Ion on Electron Beams with Solid Target Materials, Argonne Nat. Lab. Report ANL/FPP/TM-179 (1983).

[11] INTOR, Phase Two A Part 1, International Atomic Energy Agency, Vienna (1983).

[12] W.G. Wolfer and A.M. Hassanein, J. Nucl. Mater. 111/112 (1982) 560.